PAPER • **OPEN ACCESS**

Synthesis of a carbazole-substituted diphenylethylene hole transporting material and application in perovskite solar cells

To cite this article: Juncong Li *et al* 2019 *IOP Conf. Ser.: Mater. Sci. Eng.* **556** 012022

IOP Conf. Series: Materials Science and Engineering **556** (2019) 012022 doi:10.1088/1757-899X/556/1/012022

Synthesis of a carbazole-substituted diphenylethylene hole transporting material and application in perovskite solar cells

Juncong Li[1,2], Hongwei Zhu[1,2], Xianggao Li*[1,2], Shirong Wang[1,2] and Yin Xiao[1,2]

[1] Fine Chemicals Department, School of Chemical Engineering and Technology, Tianjin University, 92 Weijin Rd., Nankai Dist., Tianjin 300072, China

[2] Collaborative Innovation Center of Chemical Science and Engineering (Tianjin), 92 Weijin Rd., Nankai Dist., Tianjin 300072, China

Abstract. In this work, a carbazole-substituted stilbene derivatives hole transporting material, 9,9'-(ethene-1,1-diylbis(4,1-phenylene))bis(3,6-dimethoxy-9H-carbazole) (EPC) was designed and synthesized. The structure was characterized by FT-IR spectroscopy, ^{1}H NMR, ^{13}C NMR and MS. The glass transition temperature is 95.09°C and the 5% weight loss temperature is 423.37°C by DSC/TG analysis. Through the UV-Vis absorption spectrum combined with cyclic voltammetry, the energy level of the highest occupied molecular orbital (HOMO) of EPC and the lowest unoccupied orbital (LUMO) energy level were obtained (-5.38 eV, -2.19 eV). The energy level is well matched with methylamine lead iodine crystals. A mesoporous structure perovskite solar cell was fabricated based on the undoped EPC, and photoelectric conversion efficiency of 13.11% was obtained. After 600 hours of storage in a dark environment at 25°C and 60% relative humidity, 82% of the initial efficiency was obtained. This work provides new ideas for the development of undoped hole transporting materials.

Keywords: carbazole, hole transporting material, undoped, perovskite solar cell, stability

1. Introduce

Since 2009, organic-inorganic perovskite solar cells (PSCs) have been received attention due to their advantages in photovoltaic performance, preparation process, and cost. The highest efficiency has exceeded 22%. [1-5]

The hole transporting layer is an important structure in the perovskite solar cell and is a physical / energy barrier between the cathode and the perovskite layer, blocking the transfer of electrons to the cathode while promoting hole transporting. [6, 7] At present, the hole transporting materials for perovskite solar cells include p-type inorganic semiconductors (CuI [8], CuSCN [9], NiO [10]), polymers (P3HT [11], PTAA [12], PEDOT: PSS [13]), and organic small molecule compounds. [14-17] Because of easy purification and good film properties, triarylamine compounds are the most abundant hole transporting materials,

and the highest photoelectric conversion efficiency (PCE) is obtained in the cells using *spiro*-OMeTAD. [18] However, the cost of *spiro*-OMeTAD is high, and the use of hydrophilic dopants will affect the stability of the cells. [19] It is necessity to develop lower cost and undoped hole transporting materials.

The carbazole derivatives are excellent in charge transporting ability, have multiple reaction sites, permit fine tuning of electrical and optical properties, and are low in the price of synthetic raw materials. [20-24] Therefore, carbazole derivatives have attracted much attention as hole transporting materials. In this work, a novel carbazole-based small molecule hole transporting material is reported. Its photophysical properties are measured, a mesoporous perovskite solar cell is fabricated with an efficiency of 13.11%, in which the hole transporting material is the synthesized compound EPC.

2. Results and discussion

EPC is synthesized by nucleophilic substitution and Wittig reaction (**Scheme** S1). The molecular structure is shown in **Fig.** 1a. The structure was fully characterized by ^{1}H NMR spectroscopy, ^{13}C NMR spectroscopy and MALDI-TOF mass spectrum (**Fig.** S1-4).

Fig. 1b shows the normalized ultraviolte-visible (UV-Vis) absorption and photoluminescence (PL) spectra of EPC in tetrahydrofuran (THF) solution ($c=1\times10^{-5}$ mol/L). The maximum absorption is at 313 nm. It is caused by the π-π* transition of electrons in the molecule. [25] In addition, the EPC fluorescence emission maximum intensity is at 391 nm.

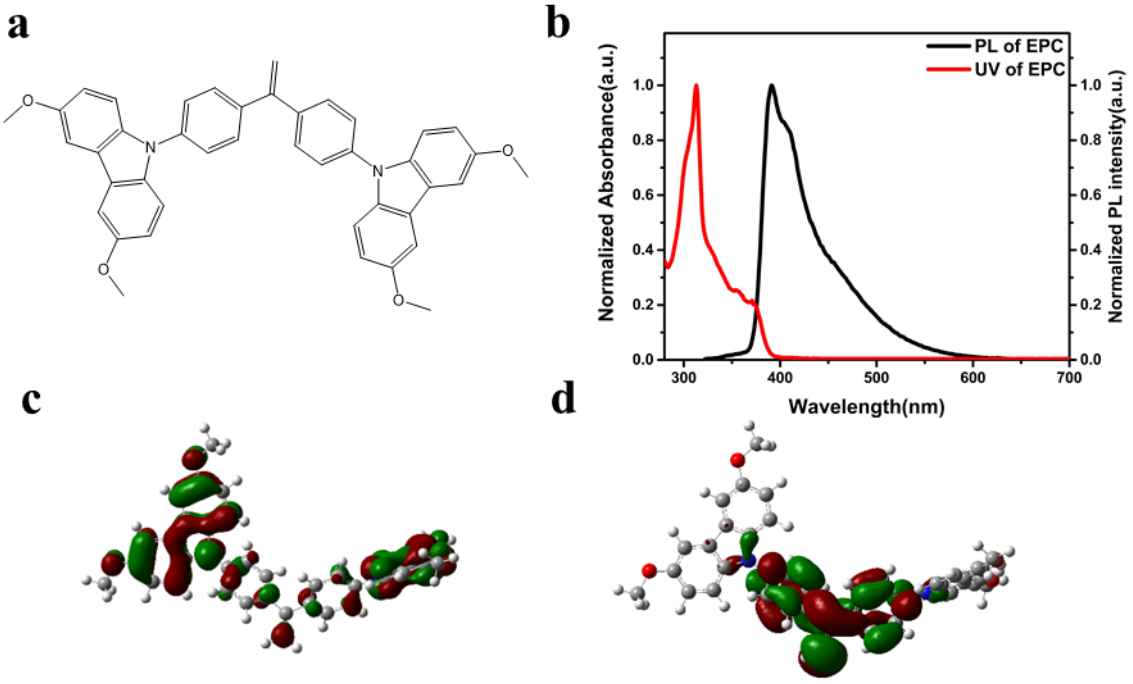

Fig. 1 (a) The molecular structure of EPC. (b) Normalized UV-Vis absorption and PL spectra of EPC in tetrahydrofuran (THF) solution. (c) HOMO distribution of EPC. (d) LUMO distribution of EPC.

In order to study the relationship between molecular structure and material properties and verify theoretically that the compound is suitable for perovskite solar cells, we used Gaussian09 calculation

software, density functional theory (DFT), B3LYP as the calculation method, and 6-31G(d) as the basis set and obtained the optimal configuration of EPC. The results are shown in **Fig.** 1c-d. Due to the presence of the rigid group carbazole, the benzene ring attached to the C=C is not coplanar, showing a rotation of 67.02˚, resulting in a large steric hindrance, not easy to form crystals, and conducive to the formation of an amorphous solid film. The highest occupied molecular orbital (HOMO) level of EPC is -4.82 eV, that mainly distributed on the benzene ring and carbazole at the periphery of the molecule. The lowest unoccupied molecular orbital (LUMO) level is -1.15 eV, that mainly distributed on the C=C in the center of the molecule and on the adjacent benzene ring, which facilitates carrier transmission.

Table 1. Photophysical, electrochemical and thermal properties of EPC

	λ_{abs} [nm]	E_g [eV]	HOMO [eV]	LUMO [eV]	T_g [℃]	T_d [℃]	μ [$cm^2 V^{-1} s^{-1}$]
EPC	313	2.05[a] 3.19[b]	-4.73[a] -5.38[b]	-1.68[a] -2.19[b]	95.09	423.37	7.23×10^{-5}

(a) calculation values (b) experiment values (HOMO level was measured by CV).

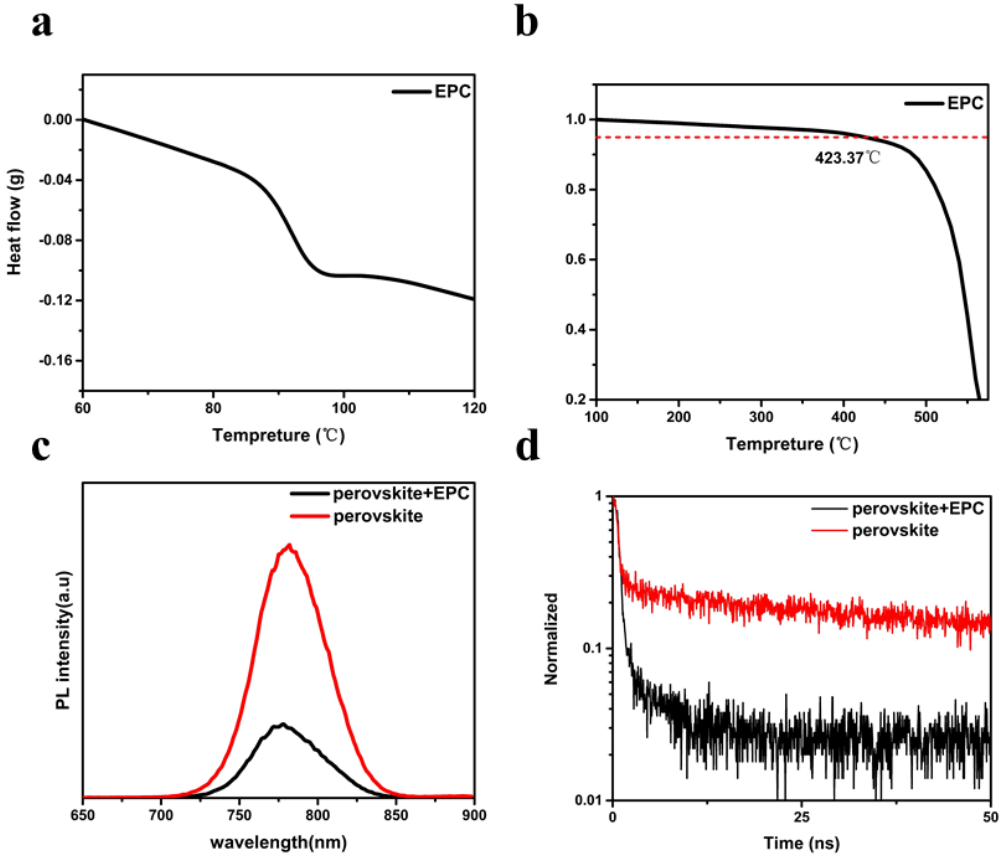

Fig. 2 (a) DSC curve. (b) TGA curve. (c) Steady-state PL spectra, excitation at 450 nm. (d) Time-resolved PL spectra, decay at 775 nm, excitation at 460 nm.

The electrical property of EPC was obtained by cyclic voltammetry (CV), and the energy levels were determined by CV and UV-Vis absorption (**Fig.** S5). The data are summarized in **Table** 1. The EPC has a HOMO energy level of -5.38 eV and a LUMO energy level of -2.19 eV. The HOMO level matches the $MAPbI_3$ HOMO level (-5.40 eV), which facilitates hole injection.

The glass transition temperature and the 5% weight loss temperature were measured by thermal gravimetric analysis (TGA) and differential scanning calorimeter (DSC), and the results are shown in **Fig.** 2a-b. The 5% weight loss temperature of EPC is 423.37 °C, and the glass transition temperature is 95.09 °C, which satisfies the application requirements of hole transporting materials for perovskite solar cells. The hole mobility of EPC was measured by space charge limited current method (SCLC). [26] The hole only device with the structure of ITO/MoO_3 (10 nm)/EPC (60 nm)/MoO_3 (10 nm)/Al (100 nm) was fabricated and the hole mobility of EPC is 7.23×10^{-5} cm^2 V^{-1} s^{-1} (**Fig.** S6).

The charge transfer process at the perovskite/EPC interface was investigated by the steady-state and time-resolved PL spectra, and the results are shown in **Fig.** 2c-d. When the EPC is deposited on top of the perovskite, the PL intensity is significantly reduced, reaching 28.41% of the perovskite film alone, indicating that between the perovskite and the EPC there is an efficient hole extraction process. [27, 28] The time-resolved photoluminescence spectra measured excitation wavelength of 460 nm and fitted the data through a double exponential decay function. Compared with the perovskite film (13.08 ns) alone, EPC can effectively reduce the fluorescence lifetime (1.17 ns). The steady state result is consistent with the PL spectrum.

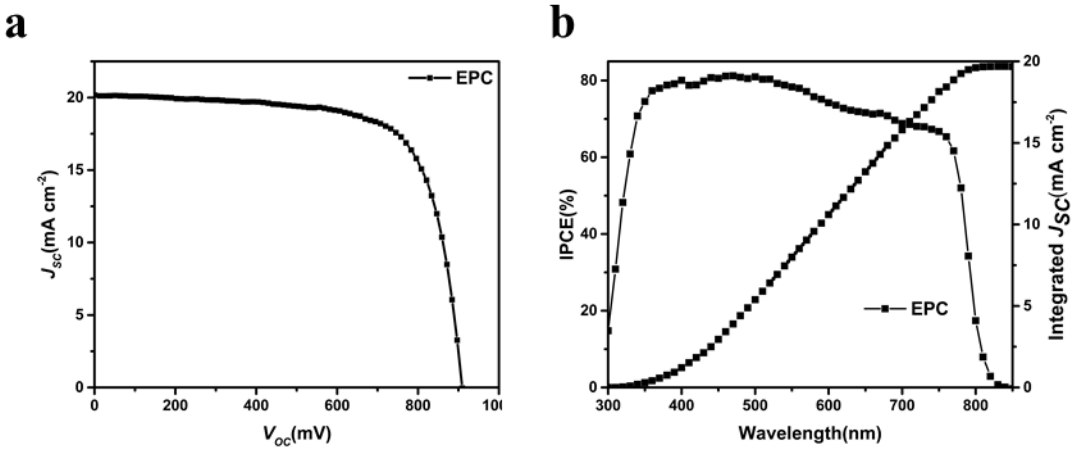

Fig. 3 (a) Current-voltage curve of perovskite solar cell based on EPC with the highest PCE. (b) IPCE spectrum and integrated current curve

Mesoporous perovskite solar cells were fabricated based on undoped EPC. The specific structure is FTO/TiO_2 compact/TiO_2 mesoporous/$MAPbI_3$/EPC/Au. The perovskite precursor solution concentration was 1.56 mol/L, the solvent was DMF/DMSO (v: v=9:1), chlorobenzene was used as the anti-solvent, and the EPC was 20 mg/mL chlorobenzene solution. The current-voltage curve (*J-V*) of cell with the highest PCE under AM 1.5 G (100 mW cm^{-2}) illumination is shown in **Fig.** 3a. The open-circuit voltage (V_{OC}) of the optimal cell is 909.43 mV and the short-circuit current (J_{SC}) is 20.17 mA cm^{-2}, the fill factor (*FF*) is 71.45%, and the photoelectric conversion efficiency (PCE) is 13.11%. In addition, **Fig.**

3b shows the incident photon current-to-electron efficiency (IPCE) spectrum of the cell based on EPC. The photocurrent density obtained from the IPCE integration is 19.68 mA cm^{-2}, which is consistent with the *J-V* curve.

Stability of EPC-based perovskite solar cells were obtained by storing cells without encapsulation in a dark state at 25 °C and 60% relative humidity and testing *J-V* curves at regular intervals. The change in PCE over time is shown in **Fig.** 4a. The test results showed that after 600 hours (25 days) of storage, the cell efficiency remained at the initial 82%. According to the previous reports, dopants can cause pinholes in the hole transporting layer and can induce decomposition of perovskite crystals. [29-31] In addition, the hydrophobic hole transporting layer can act as a barrier to decompose the perovskite of H_2O. The contact angle of the perovskite/EPC interface with water is 91.23˚, which is much larger than the contact angle of the perovskite interface with water alone. This is advantageous to block the contact between H_2O and perovskite in the air and improve the stability of the cells.

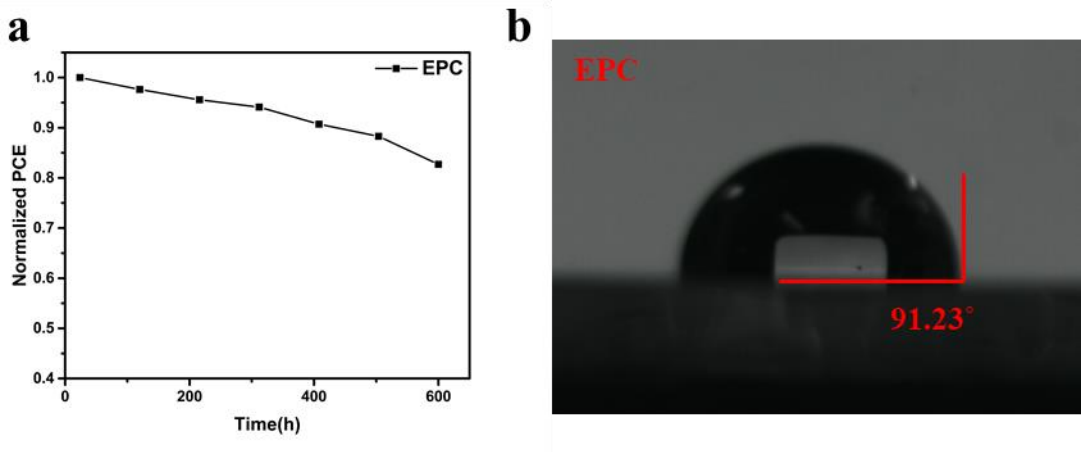

Fig. 4 (a) The stability of the cell based on EPC. (b) Contact angle between perovskite/EPC film with water in air.

3. Conclusions

In this work, a novel type of carbazole-substituted hole transporting material EPC was designed and synthesized. EPC has suitable hole mobility, good thermal stability, and energy levels that match $MAPbI_3$. The cells were fabricated based on the undoped EPC, the PCE of 13.11% was obtained, and the cell maintained its initial efficiency of 82% after 600 hours in a dark state at 25 ℃ and 60% relative humidity, showing a good stability.

4. Experiment Section

4.1. Synthesis of 3,6-dimethoxy-9H-carbazole

3,6-dibromo-9H-carbazole (6.0 g, 18.45 mmol), CuI (14.8 g, 77.50 mmol), and 70 mL DMF were charged into a three-neck flask. Methanol solution of sodium methoxide (prepared from 8.5 g, 369.5 mmol sodium and 100 mL methanol) was added under stirring and heated to reflux for 12 h. After the reaction system was cooled to room temperature, the solution was poured into 500 mL ice water to obtain a brown solid. The filter cake was filtered and washed with deionized water (3×100 mL). The

solid was separated by column chromatography (petroleum ether: ethyl acetate=10:1) to give 3.11 g white solid with a yield of 81.12%. ^{1}H NMR (400 MHz, DMSO) δ10.80 (s, 1H), 7.79 (dd, J = 102.4, 2.4 Hz, 2H), 7.33 (d, J = 8.7 Hz, 2H), 7.08–6.85 (m, 2H), 3.86 (d, J = 16.5 Hz, 6H); MS(MALDI-TOF) =226.738.

4.2. Synthesis of bis(4-(3,6-dimethoxy-9H-carbazol-9-yl)phenyl)methanone

3,6-dimethoxy-9H-carbazole (2.08 g, 9.16 mmol), t-BuNa (4.00 g, 41.60 mmol) and 40 mL DMF were charged into a two-necked flask. After argon protection, the mixture was stirred at 60℃ for 20 min, and 4,4-difluorophenone (0.95 g, 4.36 mmol) was added, then the temperature was raised to 110 ℃, and the reaction was stirred for 12 h. After the reaction system was cooled to room temperature, the solution was poured into 400 mL ice water to obtain a yellow solid. The filter cake was filtered and washed with deionized water (3×100 mL). The crude product was recrystallized from methanol and dichloromethane to give 2.01 g yellow solid with a yield of 72.57%. ^{1}H NMR (400 MHz, $CDCl_3$) δ8.24–8.00 (m, 4H), 7.76 (d, J = 8.5 Hz, 4H), 7.56 (d, J = 2.5 Hz, 4H), 7.48 (t, J = 7.7 Hz, 4H), 7.08 (dd, J = 8.9, 2.5 Hz, 4H), 3.97 (s, 12H); MS MALDI-TOF) =632.126.

4.3. Synthesis of 9,9'-(ethene-1,1-diylbis(4,1-phenylene))bis(3,6-dimethoxy-9H-carbazole)

$CH_3P^+Ph_3Br^-$ (0.84 g, 2.37 mmol) and t-BuOK (0.36 g, 3.16 mmol) were charged into a two-neck flask which was placed in ice water, and the mixture was purged with argon. The stirring was started and 50 mL dry THF was slowly added dropwise through a constant pressure dropping funnel, and the reaction was performed for 2 hours. The reaction apparatus was transferred to an oil bath, and bis(4-(3,6-dimethoxy-9H-carbazol-9-yl)phenyl)methanone (1.00 g, 1.58 mmol) was added to the reaction system, and the mixture was heated to 50 ℃ and reacted for 10 hours. After the reaction system was cooled to room temperature, the solution was poured into 400 mL ice water to obtain a yellow solid. The filter cake was filtered and washed with deionized water (3×100 mL). The solid was then separated by column chromatography (petroleum ether: ethyl acetate = 10:1), 0.65 g pale yellow solid with a yield of 65.00% was obtained. ^{1}H NMR (400 MHz, DMSO) δ 7.86 (d, J = 1.9 Hz, 4H), 7.76–7.61 (m, 8H), 7.43 (d, J = 8.9 Hz, 4H), 7.08 (dd, J = 8.9, 1.9 Hz, 4H), 5.75 (s, 2H), 3.91 (s, 12H); ^{13}C NMR (100 MHz, DMSO) δ = 56.17, 103.86, 111.07, 115.79, 116.16, 123.92, 126.40, 129,99, 135.65, 137.69, 139.33, 148.17, 154.32 ppm; MS(MALDI-TOF) =630.155.

4.4. Characterization

EPC molecular structure was identified by NMR spectroscopy and MS. We used the INOVA 400 MHz spectrometer (Varian, USA) and tetramethylsilane (TMS) as internal standards to obtain NMR spectra. MS was performed by using microTOF-QII (Bruker Daltonic, USA). The UV-Vis spectrum of EPC in THF solution ($c=1\times10^{-5}$ mol/L) was obtained by using a Thermo Evolution 300 UV-Vis spectrometer (Thermo Electron, USA). DSC and TGA were recorded under a N_2 atmosphere by using a TA Q20 (TA Instruments, USA) thermal analyzer.

The device was measured for *J-V* characteristics using 450W Xenon lamp (Oriel) at 100 mW cm^{-2}. All devices were measured by masking the active area with a metal mask with an area of 0.09 cm^2. The IPCE of the device was measured by focusing light from a 300W Xenon lamp (ILC Technology, USA) through a Gemini-180 double monochromator (Jobin Yvon Ltd., UK). TRPL and PL spectra were

measured by PL spectrometer, Edinburgh Instruments, Fluoroloy3, excited with a picosecond pulsed diode laser (EPL-460).

The CV measurements were performed on fresh dichloromethane solutions with 0.1 mol/L 1-Bu_4NPF_6 as the electrolyte by using a three-electrode system. Each solution was bubbled with Ar for 1 min before measurement. In the three-electrode system, the working electrode and the counter electrodes are Pt wires, and an Ag/0.01M $AgNO_3$ electrode (with acetonitrile as the solvent) is the reference electrode. The measurements were calibrated using ferrocene as a standard.

4.5. Device fabrication

The FTO glass was ultrasonically washed with deionized water, acetone and isopropanol successively. A titanium diisopropoxide bis(acetylacetonate) in n-butanol solution having a volume ratio of 1:16 was prepared and spin-coated at 2000 rpm for 30 s. The FTO glass was sintered at 500 ℃ for 30 min to obtain a TiO_2 compact layer. Then, a 30 nm TiO_2 ethanol suspension having a mass ratio of 1:6 was spin-coated at 5000 rpm for 30 s, and the glass was sintered at 500 ℃ for 30 min to obtain a TiO_2 mesoporous layer. The perovskite precursor solution concentration was 1.56mol/L, wherein the solvent was a DMF/DMSO mixed solution (v: v=9:1), and the perovskite spin coating process was 2000 rpm for 20 s and then 5000 rpm for 30 s. In the final 15 s of the second spin coating, 100 μL chlorobenzene solution was added dropwise, and the obtained perovskite film was annealed at 100 ℃ for 1 hour. Then, 45 μL chlorobenzene solution of EPC having a concentration of 20 mg/mL was dropwise added to the perovskite crystal layer at 4000 rpm and spin-coated for 15 s. Finally, an 80 nm gold electrode was deposited on the hole transporting layer by vacuum evaporation.

Acknowledgements

The authors gratefully acknowledge the financial support from the National Natural Science Foundation of China (21676188) and Key Projects in Natural Science Foundation of Tianjin (JCZDJC37100). The calculation in this work was supported by the high performance computing center of Tianjin University, China.

[1] Lee M M, Teuscher J, Miyasaka T, Murakami T N, Snaith H J 2012 *Science* **338** 643-7
[2] Green M A, Ho-Baillie A and Snaith H J 2014 *Nature Photonics* **8** 506-14
[3] Service R F 2011 *Science* **332** 293
[4] Williams S T, Rajagopal A, Chueh C C and Jen A K 2016 *J Phys. Chem. Lett.* **7** 811-9
[5] http://www.nrel.gov/ncpv/images/efficiency_chart.jpg
[6] Bakr Z H, Wali Q, Fakharuddin A, Schmidt-Mende L, Brown T M and Jose R 2017 *Nano Energy* **34** 271-305
[7] Zhu L, Xiao J, Shi J, Wang J, Lv S, Xu Y, Luo Y, Xiao Y, Wang S, Meng Q, Li X and Li D 2014 *Nano Research* **8** 1116-27
[8] Ye S, Rao H, Zhao Z, Zhang L, Bao H, Sun W, Li Y, Gu F, Wang J, Liu Z, Bian Z and Huang C 2017 *J Am Chem Soc* **139** 7504-12
[9] Arora N, Ibrahim D M, Hinderhofer A, Pellet N, Schreiber F, Mohammed Z S and Grätzel M 2017 *Science* **358** 768-71

[10] Xie Y, Lu K, Duan J, Jiang Y, Hu L, Liu T, Zhou Y and Hu B 2018 *ACS applied materials & interfaces* **10** 14153-9
[11] Narges Yaghoobi N, Fabio M, Lucio C, and Aldo D C 2017 *ChemSusChem* **10** 3854-60
[12] Ko Y, Kim Y, Lee C, Kim Y and Jun Y 2018 *ACS applied materials & interfaces* **10** 11633-41
[13] Xue Q, Liu M, Li Z, Yan L, Hu Z, Zhou J, Li W, Jiang X-F, Xu B, Huang F, Li Y, Yip H-L and Cao Y 2018 *Adv. Funct. Mater.* **28** 1707444
[14] Bi D, Xu B, Gao P, Sun L, Grätzel M and Hagfeldt A 2016 *Nano Energy* **23** 138-44
[15] Xu B, Bi D, Hua Y, Liu P, Cheng M, Grätzel M, Kloo L, Hagfeldt A and Sun L 2016 *Energy Environ. Sci.* **9** 873-7
[16] Gratia P, Magomedov A, Malinauskas T, Daskeviciene M, Abate A, Ahmad S, Gratzel M, Getautis V and Nazeeruddin M K 2015 *Angew. Chem. Int. Ed. Engl.* **54** 11409-13
[17] Xu B, Zhang J, Hua Y, Liu P, Wang L, Ruan C, Li Y, Boschloo G, Johansson E M J, Kloo L, Hagfeldt A, Jen A K Y and Sun L 2017 *Chem* **2** 676-87
[18] Yu Z and Sun L 2015 *Adv. Energy Mater.* **5** 1500213
[19] Rakstys K, Saliba M, Gao P, Gratia P, Kamarauskas E, Paek S, Jankauskas V and Nazeeruddin M K 2016 *Angew. Chem. Int. Ed. Engl.* **55** 7464-8
[20] Xu B, Sheibani E, Liu P, Zhang J, Tian H, Vlachopoulos N, Boschloo G, Kloo L, Hagfeldt A and Sun L 2014 *Adv. Mater.* **26** 6629-34
[21] Magomedov A, Paek S, Gratia P, Kasparavicius E, Daskeviciene M, Kamarauskas E, Gruodis A, Jankauskas V, Kantminiene K, Cho K T, Rakstys K, Malinauskas T, Getautis V and Nazeeruddin M K 2018 *Adv. Funct. Mater.* **28** 1704351
[22] Li D, Shao J Y, Li Y, Li Y, Deng L Y, Zhong Y W and Meng Q 2018 *Chem. Commun. (Camb.)* **54** 1651-4
[23] Benhattab S, Cho A-N, Nakar R, Berton N, Tran-Van F, Park N-G and Schmaltz B 2018 *Org. Electron.* **56** 27-30
[24] Daskeviciene M, Paek S, Wang Z, Malinauskas T, Jokubauskaite G, Rakstys K, Cho K T, Magomedov A, Jankauskas V, Ahmad S, Snaith H J, Getautis V and Nazeeruddin M K 2017 *Nano Energy* **32** 551-7
[25] Qi P, Zhang F, Zhao X, Liu X, Bi X, Wei P, Xiao Y, Li X and Wang S 2017 *Energy Technology* **5** 1173-8
[26] Kwon O K, Uddin M A, Park J H, Park S K, Nguyen T L, Woo H Y and Park S Y 2016 *Adv. Mater.* **28** 910-6
[27] Roldán-Carmona C, Gratia P, Zimmermann I, Grancini G, Gao P, Graetzel M and Nazeeruddin M K 2015 *Energy Environ. Sci.* **8** 3550-6
[28] Mosconi E, Grancini G, Roldán-Carmona C, Gratia P, Zimmermann I, Nazeeruddin M K and De Angelis F 2016 *Chem. Mater.* **28** 3612-5
[29] Li W, Dong H, Wang L, Li N, Guo X, Li J and Qiu Y 2014 *J. of Mater. Chem. A* **2** 13587-92
[30] Hawash Z, Ono L K, Raga S R, Lee M V and Qi Y 2015 *Chem. Mater.* **27** 562-9
[31] Berhe T A, Su W-N, Chen C-H, Pan C-J, Cheng J-H, Chen H-M, Tsai M-C, Chen L-Y, Dubale A A and Hwang B-J 2016 *Energy Environ. Sci.* **9** 323-56

IOP Conf. Series: Materials Science and Engineering **556** (2019) 012022 doi:10.1088/1757-899X/556/1/012022

Supporting information

Synthesis of a carbazole-substituted diphenylethylene hole transporting material and application in perovskite solar cells

Juncong Li[1,2], Hongwei Zhu[1,2], Xianggao Li*[1,2], Sshirong Wang[1,2] and Yin Xiao[1,2]

[1] Fine Chemicals Department, School of Chemical Engineering and Technology, Tianjin University, 92 Weijin Rd., Nankai Dist., Tianjin 300072, China

[2] Collaborative Innovation Center of Chemical Science and Engineering (Tianjin), 92 Weijin Rd., Nankai Dist., Tianjin 300072, China

1. synthesis route

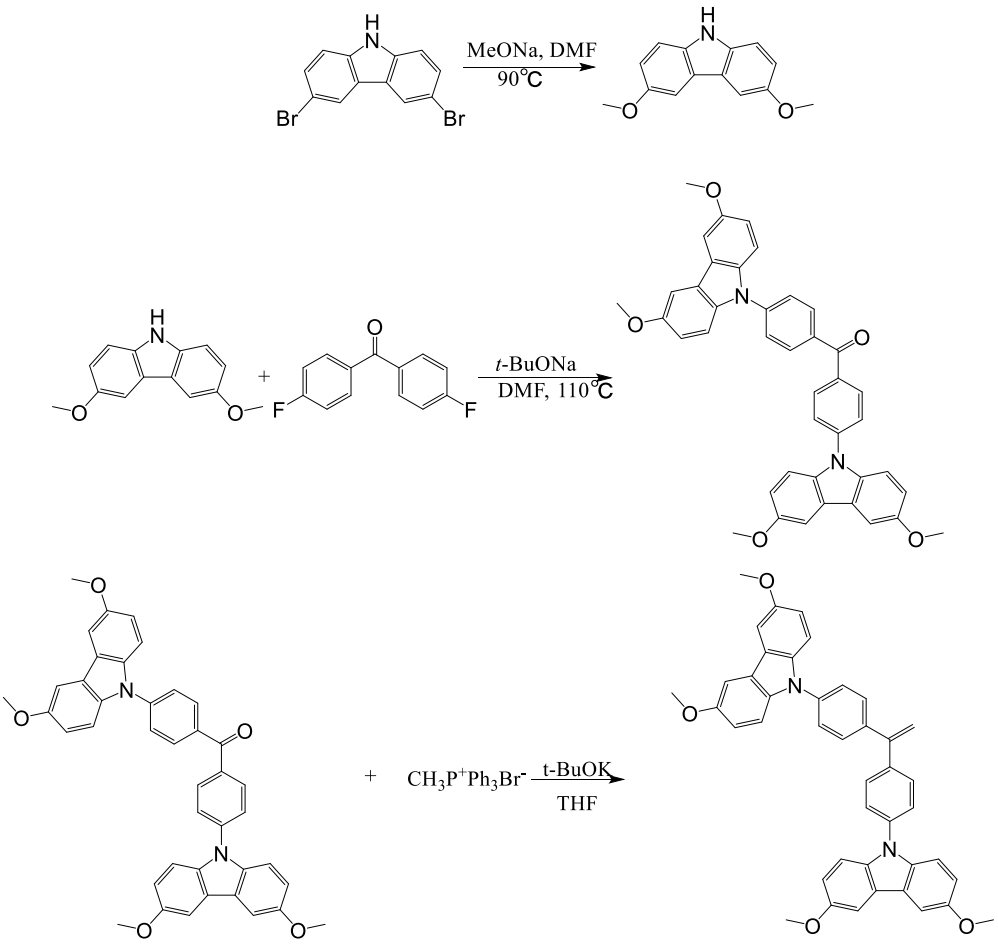

Scheme S1 Outline of synthesis of EPC.

2. Structural characteristics

The structure of synthesized compounds 1 were confirmed *via* ^{1}H NMR and ^{13}C NMR, which agreed well with the proposed molecular structure.

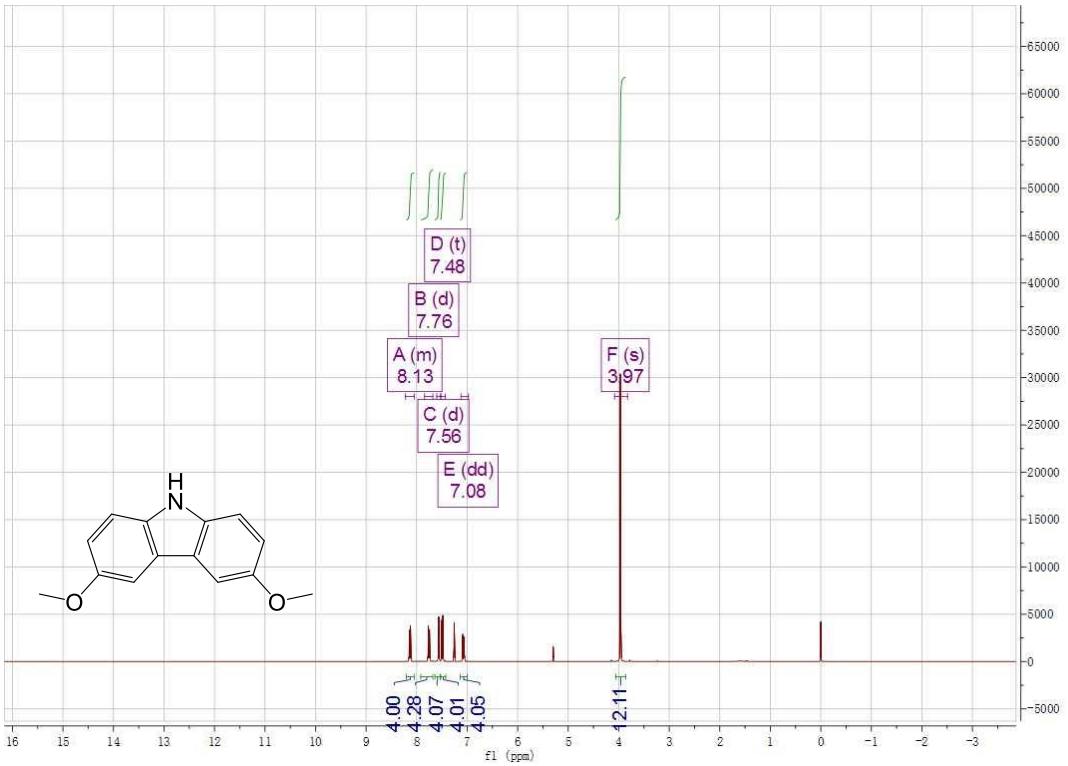

Fig. S1 [1]H NMR of 3,6-dimethoxy-9H-carbazole.

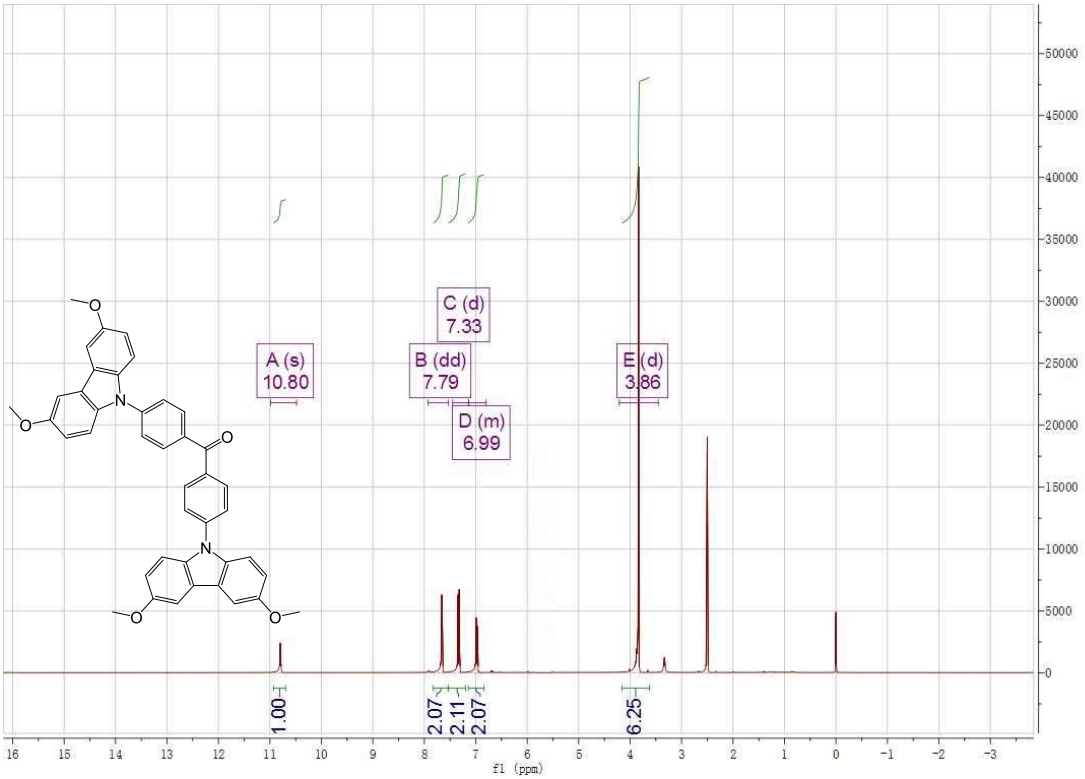

Fig. S2 [1]H NMR of bis(4-(3,6-dimethoxy-9H-carbazol-9-yl)phenyl)methanone.

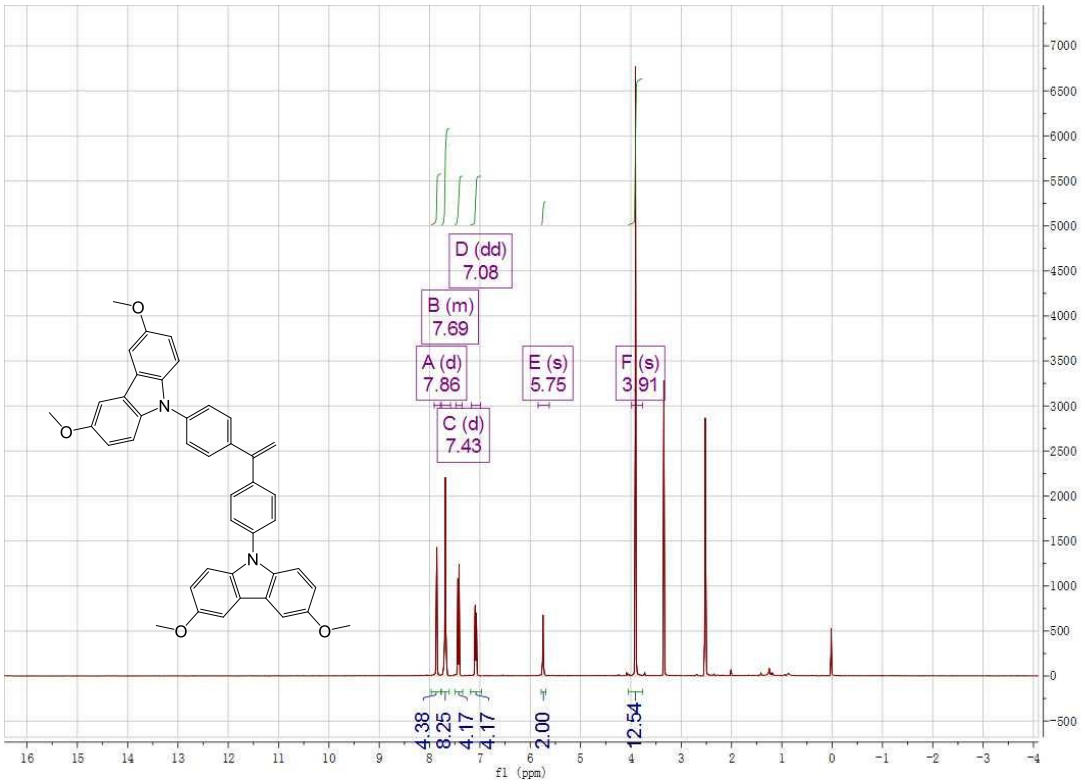

Fig. S3 ^{1}H NMR of EPC.

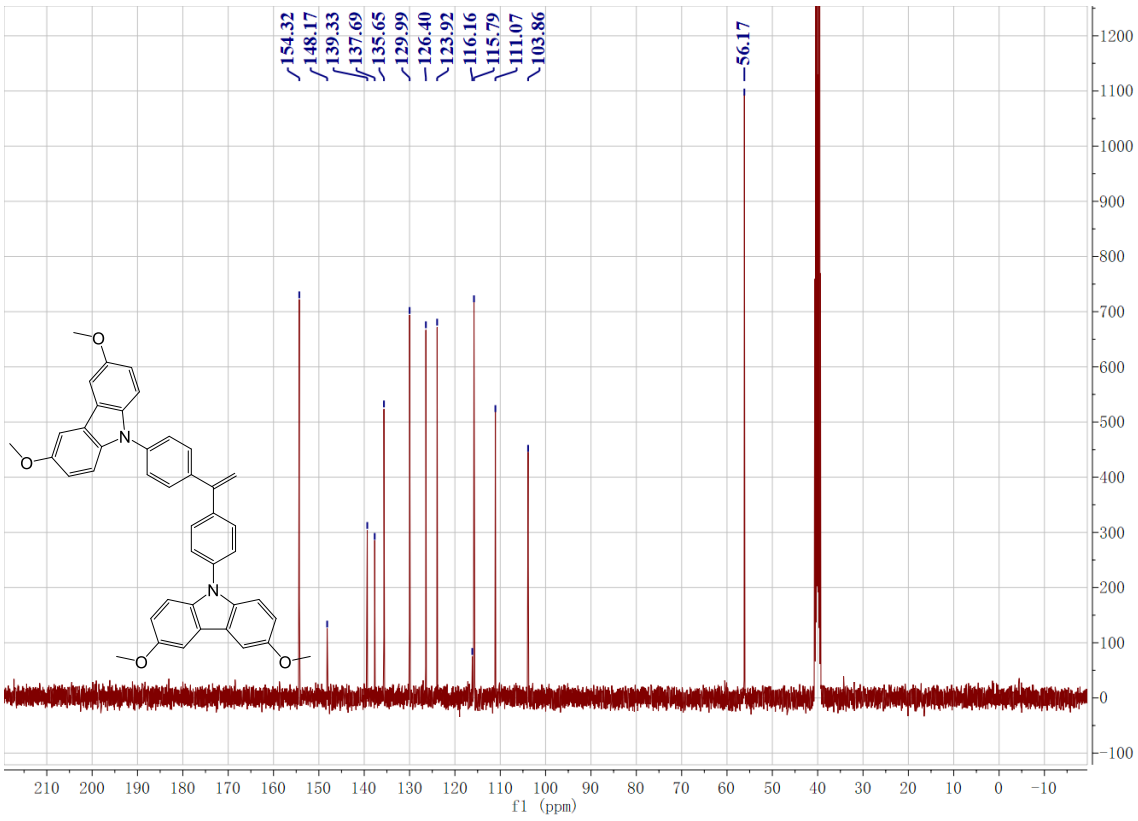

Fig. S4 ^{13}C NMR of EPC

3. cyclic voltammetry

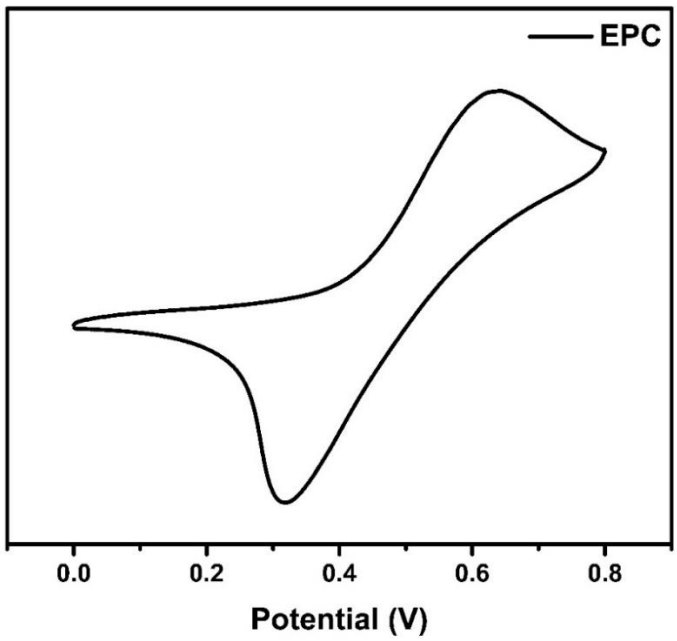

Fig. S5 Cyclic voltammetry curve of EPC.

4. Hole transporting mobility measurement

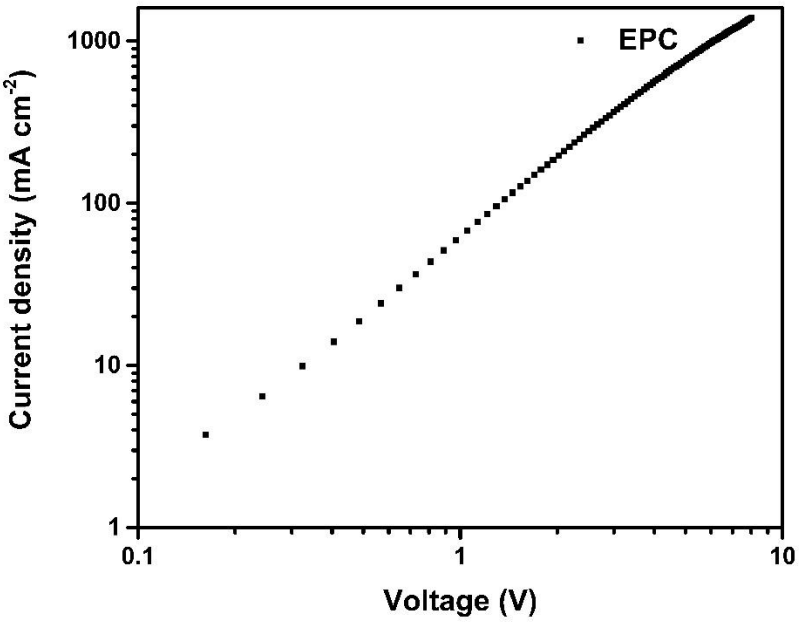

Fig. S6 *J-V* curve by SCLC